

X-ray Industrial Computed Laminography (ICL) Simulation Study of Planar Objects: Optimization of Laminographic Angle

*Lakshminarayana Yenumula**, Umesh Kumar, and Ashutosh Dash

*Industrial Tomography and Instrumentation Section, Isotope Production and Applications
Division, Bhabha Atomic Research Centre, Mumbai – 400085, India
91 22 2559 0180, laxmany@barc.gov.in*

Abstract

X-ray Industrial Computed Laminography (ICL) is a non-destructive three-dimensional (3D) imaging technique for high aspect ratio planar objects such as printed circuit boards and stacked IC. Complementing to the established method of X-ray Industrial Computed Tomography (ICT), ICL is based on tilt orientation of the planar object with respect to incident X-ray beam by a defined angle. The tilt angle of the planar object is called laminographic angle. Knowledge about the laminographic angle is very important for optimizing reconstruction quality of planar objects. This paper presents optimization of laminographic angle using simulated planar object in cone-beam geometry. Root Mean Square (RMS) contrast is used to characterize the effect of the angle on reconstruction quality. Simulated cone-beam projections (radiographs) were generated from different angles by rotating tilted planar object. FDK (Feldkamp, Davis and Kress) reconstruction algorithm has been adapted to reconstruct the planar object from the radiographs. Best reconstruction results are obtained when an optimal laminographic angle of 45 degree is used for data acquisition. The simulation study can be employed for in situ testing of planar specimens.

Keywords: X-ray Industrial Computed Laminography (ICL), Non-destructive, X-ray Industrial Computed Tomography (ICT), RMS contrast, FDK reconstruction algorithm.

1. Introduction

X-ray Industrial Computed Tomography (ICT) is an established three-dimensional (3D) imaging non-destructive testing (NDT) method for industrial applications. Industrial applications include manufacturing industry and other industries, e.g., food, electrical and electronics industries [1]. However, when planar objects with high aspect ratio (area-to-thickness) like printed circuit boards to be inspected with high resolution, ICT has its limitations. When the planar object is examined in CT, x-ray absorption in the object increases drastically along the longitudinal direction. This limited transmission generates very noisy radiographs at these angles, which leads to artefacts in reconstruction. Other drawback includes geometrical

restriction that does not allow long planar object to move close to source for getting high resolution. Industrial Computed Laminography (ICL) provides an alternative to ICT to overcome these limitations. Applications for CL are relatively new in industrial non-destructive testing [2-5], at least if one compares the situation to well established ICT. Some of these CL applications are X-ray micro- and nano-imaging [6-9] and neutron imaging [10].

The geometry of ICL measurements is different from ICT measurements. Object is rotated around an axis that is perpendicular to the X-ray beam direction during tomographic measurements, whereas planar object is tilted by an angle smaller than 90 degrees such that the normal to its large plane is not parallel to the incident beam in ICL. The tilt angle of the planar object is called laminographic angle. This angle gives additional degree of freedom which makes laminography flexible to image specimens that have two dimensions larger than third one [11]. Hence laminographic data acquisition scheme provides more reliable projection data than tomography when a planar object is scanned. Knowledge about the laminographic angle is very important for optimizing reconstruction quality of planar objects. The present work aims at optimization of laminographic angle with simulated high aspect ratio planar object. Root Mean Square (RMS) contrast is used to characterize the effect of the tilt angle on reconstruction image quality. The paper also describes the reconstruction of planar object, which includes generation of phantom (planar object) and simulation of radiographs.

The organization of the paper is as follows: Section 2 describes laminographic data acquisition and evolution metrics. Data collection parameters and simulation results have been discussed in Section 3. Conclusions are given in Section 4.

2. Laminographic Imaging in Cone-beam Geometry

Laminographic imaging has different acquisition geometries. Early approaches simply integrate an image during a synchronized motion of the source and detector in order to blur out specimen features that are not situated on the so-called focal plane of the apparatus. Other acquisition schemes use a divergent (fan- or cone-beam) geometry to acquire different projection images from different angles that are combined in a reconstruction step to yield cross-sectional or 3D images. The cone-beam acquisition scheme is implemented in this study. Figure 1 shows the comparison of tomography and laminography scanning geometries in cone-beam geometry. The image acquisition scheme shown is relatively ease due to the requirement of one rotation. Like ICT imaging, ICL imaging setup also consists of three parts: an X-source, a 2D flat panel detector, and a test object. Both source and detector are stationary. Projection images are acquired on the 2D flat panel detector under rotation of the object by a defined tilt angle. The principle difference of ICL compare to ICT is that the rotation axis is inclined at an angle less than 90 degrees with respect to the direction of the cone-beam optical axis.

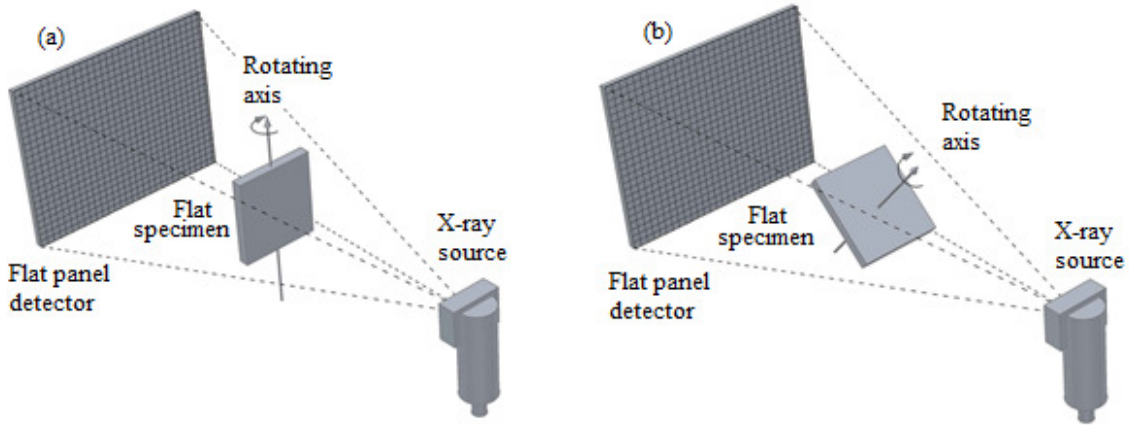


Figure 1: Schematic representation of ICT and ICL scanning geometries in cone-beam geometry. (a) ICT geometry where tomographic rotation axis is perpendicular with respect to the beam direction. (b) ICL geometry where tomographic rotating axis is inclined by a defined laminographic angle with respect to the beam direction.

2.1 Evaluation metrics

For quantitative evaluation of speed of the simulation process and optimization of laminographic angle, two numerical indices have been used. One is the average time, t_{avg} and the other is Root Mean Square (RMS) contrast. The average time measures the efficiency of projection and backprojection implementation by computing the average time that is required to process all voxels for generation of radiographs and reconstruction of 3D data. The second index, RMS contrast is related to the quality of reconstruction which is influenced by the object tilt angle. It is the difference in visual properties that makes a feature in a reconstructed image distinguishable from other feature and the background noise. RMS contrast is defined as the standard deviation or reconstruction noise of the pixel values [12]:

$$\text{RMS contrast} = \sqrt{\frac{1}{MNP} \sum_{i=0}^{M-1} \sum_{j=0}^{N-1} \sum_{k=0}^{P-1} (f(i, j, k) - \bar{f})^2} \quad (1)$$

Where $f(i, j, k)$ is the intensity of i -th, j -th and k -th elements of three-dimensional image of size M by N by P and \bar{f} is the average intensity of all pixel values in the image.

3. Simulation Results

The cone-beam ICL simulation setup consists of three parts: an X-source, a 2D flat panel detector and a test object. The test object used for the study is a planar object having high aspect ratio (area-to-thickness) of 60 (figure 2(a)). Although in reality X-ray source produces multi-energy rays, we assumed the cone-beam has single-energy rays in the simulation. The flat panel detector consists of a pixel array with 512 pixels both in rows and columns. The influence of other physical effects like scatter radiation and noise are ignored. Data acquisition was

performed with a source-to-detector distance of 1000 mm, a magnification of 2 and tilt angle ranging from 5 to 60 degree with a step size of 5 degree. 100 cone-beam simulation projections (radiographs) of 256 x 256 pixels were acquired over 360 degree with a step size of 3.6 degree. The radiographs were calculated using an analytical ray tracing approach. FDK (Feldkamp, Davis and Kress) reconstruction algorithm based on circular orbit scanning was then adapted for reconstruction of 3D volume from the radiographs. The reconstruction of simulated object contains 64 x 64 x 64 pixels. To this end, in-house developed imaging software module has been used. This software tool is dedicated for simulation of ICL imaging technique. It consists of three components: generation of projection images (radiographs), reconstruction and visualization. Figure 4 shows different slices through the reconstructed 3D data of simulated planar object.

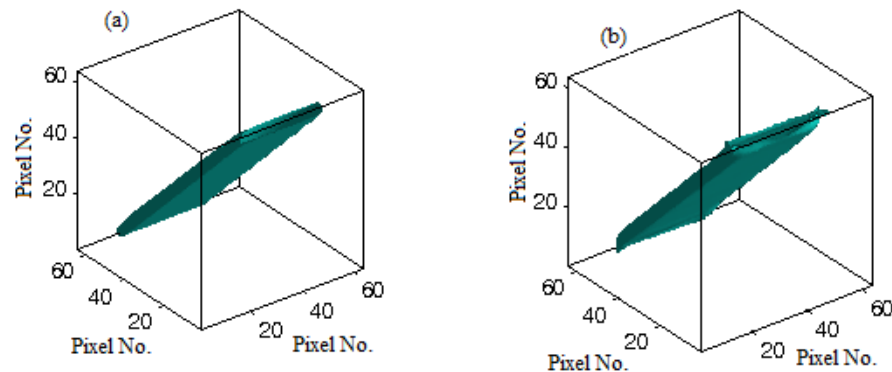


Figure 2: (a) The phantom used for the study is a high aspect ratio planar object (b) Reconstructed 3D volume of the planar object contains 64^3 voxels.

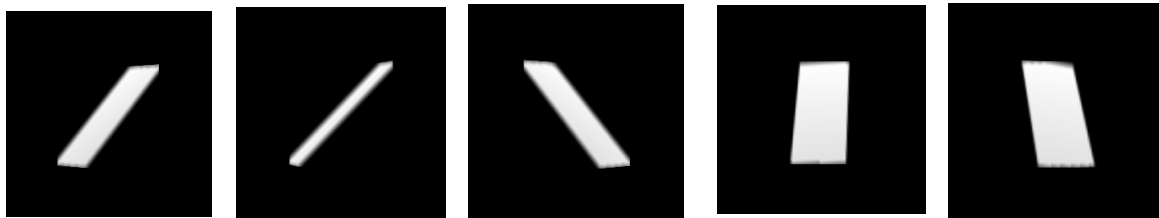


Figure 3: Simulated cone-beam projections (radiographs) of the planar object under different scan angles.

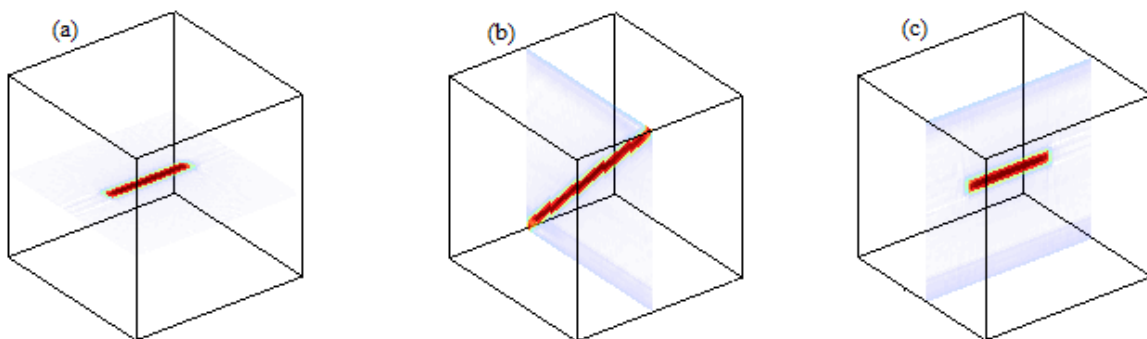


Figure 4: Different slices through reconstructed 3D data of the planar object. (a) Slice cut through x-y plane (b) Slice cut through y-z plane (c) Slice cut through x-z plane

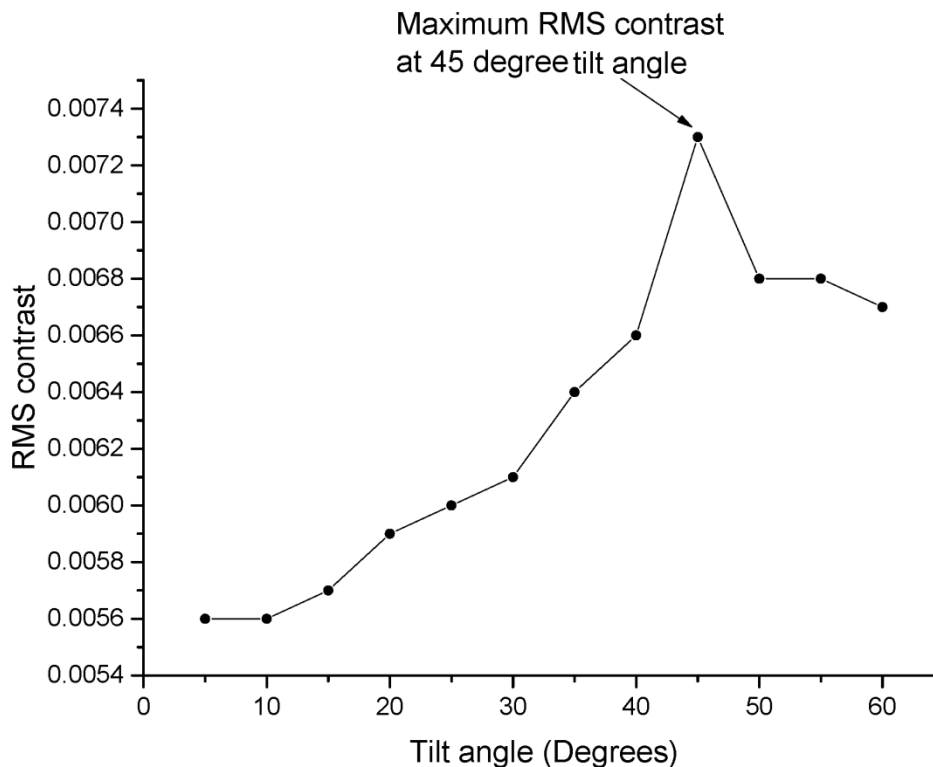


Figure 5: Plot of RMS contrast as a function of tilt angle

To study the influence of tilt angle on the reconstruction quality, Root Mean Square (RMS) contrast was used. Figure 5 corresponds to plot of RMS contrast as function of laminographic angle. The RMS contrast increases with increasing laminographic angle and reaches maximum at tilt angle 45 degree and then decreases. Hence reconstructed image of the 45 degree tilt angle offers a better contrast than the other tilt angles.

4. Conclusions

In this paper laminographic angle is optimized for simulated high aspect ratio planar object. Root Mean Square (RMS) contrast has been used as a quantitative metric to characterize the effect of the angle on reconstruction quality. Simulation results have shown that optimum reconstruction values are obtained for laminographic angle of 45 degree. If we use the optimum tilt angle during laminographic data acquisition, contrast of reconstructed planar objects can be increased. The simulation study can be employed for in situ testing of planar specimens. Implementation of three-dimensional iterative reconstruction algorithms will be the working emphasis in next phase as a way to provide good quality reconstruction of planar objects from a small number of projections.

Acknowledgments

The authors acknowledge Dr. K.L. Ramakumar, Director, Radiochemistry and Isotope Group, BARC for his support and encouragement.

References

1. L. De Chiffre., S. Carmignato., J.-P. Kruth., R. Schmitt., A. Weckenmann. "Industrial Applications of Computed Tomography," *CIRP Ann.-Manuf. Technol.* 63: 655–677 (2014).
2. A. Kalukin and V. Sankaran, "Three-dimensional visualization of multilayered assemblies using X-ray laminography," *IEEE T. Compon. Pack. A* 20, 361–366 (2002).
3. T. Moore, D. Vanderstraeten, and P. Forssell, "Three-dimensional x-ray laminography as a tool for detection and characterization of BGA package defects," *IEEE Compon. Pack. T* 25, 224–229 (2002).
4. S. Rooks, B. Benhabib, and K. Smith, "Development of an inspection process for ball-grid-array technology using scanned-beam X-ray laminography," *IEEE. Compon. Pack. A* 18, 851–861 (2002).
5. V. Sankaran, A. Kalukin, and R. Kraft, "Improvements to X-ray laminography for automated inspection of solder joints," *IEEE Compon. Pack. C* 21, 148–154 (2002).
6. F. Xu, L. Helfen, A. Moffat, G. Johnson, I. Sinclair, and T. Baumbach, "Synchrotron radiation computed laminography for polymer composite failure studies," *J. Synchrotron Radiat.* 17, 222–226 (2010).
7. L. Helfen, A. Myagotin, P. Pernot, M. DiMichiel, P. Mikul'ik, A. Berthold, and T. Baumbach, "Investigation of hybrid pixel detector arrays by synchrotron-radiation imaging," *Nucl. Instrum. Meth. A* 563, 163–166 (2006).
8. F. Xu, L. Helfen, H. Suhonen, D. Elgrabli, S. Bayat, P. Reischig, T. Baumbach, and P. Cloetens, "Correlative nanoscale 3d imaging of structure and composition in extended objects," (2011).
9. T. Tian, F. Xu, J. Kyu Han, D. Choi, Y. Cheng, L. Helfen, M. Di Michiel, T. Baumbach, and K. N. Tu, "Rapid diagnosis of electromigration induced failure time of pb-free flip chip solder joints by high resolution synchrotron radiation laminography," *Appl. Phys. Lett.* 99, 082114 (2011).
10. L. Helfen, F. Xu, B. Schillinger, E. Calzada, I. Zanette, T. Weitkamp, and T. Baumbach, "Neutron laminography– a novel approach to three-dimensional imaging of flat objects with neutrons," *Nucl. Instrum. Meth. A* (2011).
11. Xu F, Helfen L, Baumbac T, Suhonen H, "Comparison of image quality in computed laminography and tomography," *Opt Express* 20: 794-806 (2012).
12. R. Gholipour-Peyvandi , S.Z. Islami-Rad, R. Heshmati, S. Zaferanlouie, and M. Ghannadi-Maragheh, "Influence of gamma energy on the image contrast for material with different density," *International Journal of Pure and Applied Physics*, vol. 42 (3-4), pp. 425-431, (2011).